Bibliographical reference

Source Localization Using Multi-Path Time Delays Measured by Two Hydrophones in the Deep Ocean, Ran Cao, Kunde Yang, Yuanliang Ma, Qiulong Yang, Huijun Xia and Yang Shi, Acta Acustica **vol. 105** (Number 1), 2019, pp. 248-252

DOI

https://doi.org/10.3813/AAA.919306

ACTA ACUSTICA UNITED WITH ACUSTICA
Vol. 105 (2019) 248 – 252

DOI 10.3813/AAA.919306

Source Localization Using Multi-Path Time Delays Measured by Two Hydrophones in the Deep Ocean

Ran Cao, Kunde Yang, Yuanliang Ma, Qiulong Yang, Huijun Xia, Yang Shi

[1] School of Marine Science and Technology, Northwestern Polytechnical University, Xi'an 710072, China. ykdzym@nwpu.edu.cn

[2] Key Laboratory of Ocean Acoustics and Sensing (Northwestern Polytechnical University), Ministry of Industry and Information Technology, Xi'an 710072, China

Summary

In this paper, an efficient source location approach based on the time delay between bottom-surface reflection and surface-bottom reflection (TDBS) in the deep ocean was proposed. The source range and depth were derived with the TDBSs and the corresponding receiver depths on the basis of ray theory. For a single receiver, the relationship between the TDBS and the source position could be regarded as a monotonic function, which corresponded to the main lobe on the ambiguity surface calculated by matching the multipath time delays of the real data and the replicas. The source could be localized by the intersection of the main lobes, which were calculated using the TDBSs measured by at least two receivers. The performance was demonstrated with numerical simulation and experiments for the source in and out of the shadow zone.

PACS no. 43.30.Cq, 43.30.Pc, 43.60.Kx

1. Introduction

The passive source location method has been researched for decades and extensively applied to the signal processing in underwater acoustics, including the monitoring of marine mammals, and the localization of ships and autonomous underwater vehicles. In recent years, passive source localization has been attained by different monitoring systems, such as a single array, a single hydrophone, multiple arrays, distributed hydrophones, and a combination of arrays and distributed hydrophones.

The estimations of source positions in the deep ocean mainly rely on the time difference of arrivals (TDOA) and the coherent structure (acoustic interference) at hydrophones. Tenorio-Hallé *et al.* introduced the "double-difference" method from seismology and it is based on the difference in elevation angle and time delay arrivals between multiple eigenrays.[1] The moving source can be tracked by a single vertical line array in the deep water SOFAR channel. Matched multipath time arrivals were proposed for three-dimensional localization in the azimuthally dependent oceanic environment with one or two hydrophones [2, 3]. Using the depth-dependent interference between the direct and surface-reflected(D-SR) arrivals with a vertical array in the reliable acoustic path, Mccargar and Zurk proposed a depth-based signal separation (DBSS) method where the source depth can be passively estimated by a modified Fourier transform to the power output of the vertical beamformer [4]. Further, Kniffin *et al.* analyzed the performance of the DBSS and introduced a depth estimation method by measuring the null spacing in the interference structure [5]. On the basis of the D-SR time delays, Duan *et al.* adopted an extended Kalman filter to estimate the moving source position and speed by a single hydrophone [6]. Techniques such as relative time delays with a Bayesian scheme or a matched cross-correlation function between the D-SR arrivals at two hydrophones were adopted in the deep ocean [7, 8]. The bottom-surface(BS) and surface-bottom(SB) arrivals are chosen for localizing the source in the shadow zone, where the D-SR arrivals do not exist on the basis of ray theory. Yang *et al.* presented a source depth estimation approach based on the time delays of bottom reflection (BR) and surface-bottom-surface(SBS) reflection or SB reflection and BS reflection with a vertical line array at moderate range in the deep ocean [9, 10]. Weng *et al.* presented a passive source localization method with a single hydrophone based on the interference of periodic structures matched with modeled interference stripes, which are dominated by BR, SBS, SB and BS rays [11]. Duan *et al.* proposed a narrowband source localization method, in which the source range and depth are estimated by the weighted subspace fitting technique and the time delays between BR and SB arrivals [12].

In this paper, the source range and depth are shown to be connected with the time delay between BS and SB (TDBS) arrivals. The source position can be localized by comparing the simulated and measured TDBS arrivals at two vertically aligned hydrophones. The remainder of this paper is organized as follows. Section 2 describes the relationship between the TDBS and the source position. Section 3 presents the numerical simulation to demonstrate the performance of the TDBS method in the deep ocean. Section 4 shows the experimental results with the TDBS method in the South China Sea. The conclusion of this work is drawn in the final section.

2. Description of the source localization method

For simplicity, a deep ocean waveguide with a bilinear sound speed profile (SSP) was considered, as shown schematically in Figure 1. The SSP can be expressed as

$$c(z) = c_0 g_i \left| z_c - z \right|, \quad g_i \le 0, \quad i = 1, 2, \tag{1}$$

where g_i, z_c and c_0 represent the sound speed gradient above or below the axis of the sound channel and the depth and sound speed of the sound channel, respectively.

The travel time of a given ray can be simplified as [13]

$$t(z) = \int_{z_0}^{z} \frac{1}{c(z')\sqrt{1 - a^2 c^2(z')}} \, \mathrm{d}z', \tag{2}$$

where z_0 is the source depth, $ac = k_r c/\omega = k_r (k = \cos\theta$, and θ represents the ray declination angle at any depth. By combining Equations (1) and (2), the travel time can be expressed by the grazing angle [14],

$$\begin{aligned} t(\theta) &= \frac{1}{g_i} \left| \int_{\theta_i}^{\theta_{i+1}} \frac{1}{\cos\phi} \, \mathrm{d}\phi \right| \\ &\approx \sum_i \frac{1}{g_i} \left| 2\theta_i - 2\theta_{i-1} + \theta_i^3/3 - \theta_{i-1}^3/3 \right|. \end{aligned} \tag{3}$$

Based on Snell's Law, the relationship between the grazing angle and the sound speed can be expressed as $\cos\alpha_{BS}/c_s = a_{BS}$ and $\cos\alpha_{SB}/c_s = a_{SB}$, where α_{SB} and α_{BS} represent the grazing

Received 3 June 2018,
accepted 6 December 2018.

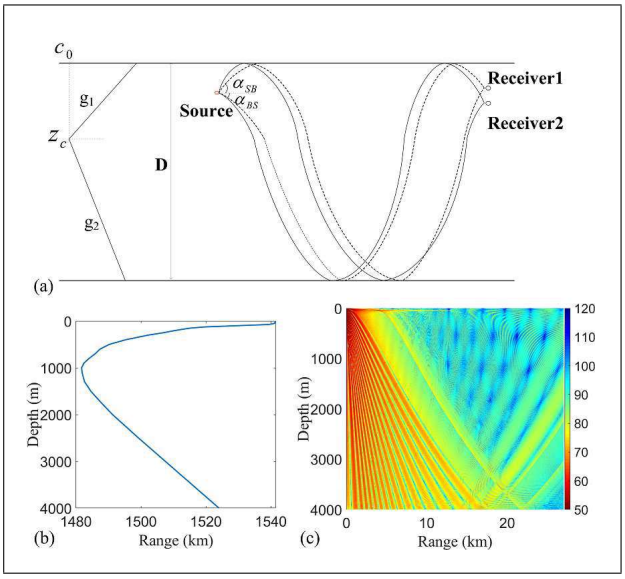

Figure 1. Schematic of the BS and SB paths in an ocean waveguide and the measured SSP (a) bilinear SSP and the source/receivers above the sound channel axis, (b) the measured SSP in the experiment and (c) corresponding transmission loss at 250 Hz with the source at 50 m using BELLHOP.

angles for the SB and BS paths, respectively, α_{BS} and α_{SB} are constants, and c_s is the sound speed at the source depth. By expanding the grazing angle in a Taylor series and neglecting the high order terms, the travel time along the BS and SB paths can be expressed as

$$\begin{aligned} t_{BS} &\approx a_{BS}\frac{16-8\pi}{\pi^2-8}\left(4D-2z_s+2z_r\right), \\ t_{SB} &\approx a_{SB}\frac{16-8\pi}{\pi^2-8}\left(4D+2z_s-2z_r\right), \end{aligned} \tag{4}$$

where D, z_s and z are the waveguide depth, source depth and receiver depth, respectively, as shown in Figure 1. Similarly, the horizontal distance in the stratified medium with the same sound speed gradient can be written as

$$\begin{aligned} r(z) &= \sum_i \frac{1}{ag_i}\left|\int_{\theta_i}^{\theta_{i+1}}\cos\phi\,\mathrm{d}\phi\right| \\ &\approx r(z_0)+\sum_i \frac{1}{ag_i}\left|\theta_i-\theta_{i-1}-\left(\theta_i^3/3-\theta_{i-1}^3/3\right)\right|. \end{aligned} \tag{5}$$

Considering that the declination angles along each path are small for a large propagation range, the relationship between the travel time and the horizontal distance can be approximated as $t \approx 2a\big(r(z)-r(z_0)\big)$ from Equations (3) and (5). By differentiating r and t with respect to θ, $u = (\partial r/\partial\theta)/(\partial t/\partial\theta) = \partial r/\partial t$ is a constant as the wave propagates along the ray. The horizontal distances covered by the BS and SB paths are the same as shown in Figure 1a. Substituting Equations (4) and (5) into the above approximation relation between the travel time and the horizontal distance, the constraint condition was concluded to be $2D \ll |z_r - z|$ [10]. In other words, the TDBS method can be utilized under the assumption that the difference between the source and the receiver depths can be neglected compared with the waveguide depth.

Notably, TDBS can be related to the horizontal distance and the receiver depth from Equations (4) and (5). The relationship can be expressed as

$$\begin{aligned} \tau_{BS-SB} &= \left(t_{BS}-t_{SB}\right) = 2\left(a_{BS}+a_{SB}\right)r \\ &= \frac{32-16\pi}{\pi^2-8}\Big[2D\left(a_{BS}-a_{SB}\right) \\ &\qquad +\left(a_{BS}+a_{SB}\right)\left(z_r-z_s\right)\Big]. \end{aligned}$$

This relationship directly indicates that TDBS has a unique solution when the horizontal distance, source and receiver depth are fixed. The TDBSs calculated for the receivers at different depths are different. The relationship between the TDBS and the source position is regarded as a monotonic function in Equation (6). The simulated TDBSs on a hydrophone at depths of 50 m and 300 m are shown in Figure 2a and 2b, respectively. Comparing the results in the Figure 2a and 2b, the TDBSs are different for the hydrophone at a given position, which are calculated from two different sources. The TDBS is more sensitive to the depth variation than to the range variation when the receiver depth is closer to the source depth, and vice versa. Therefore, the source position can be estimated by matching the TDBSs of the real data and the replicas, which are calculated from at least two hydrophones at different depths.

By using the least square errors between the measured and modeled TDBSs, the cost function is defined as

$$L(s) = \prod_i^N \max\left[\exp\left(\frac{-1}{2\sigma^2}\left(\tau_r(i)-\tau_m(s)\right)^2\right)\right], \tag{6}$$

where $\tau_r(i)$ is the measured TDBS at the ith receiver, N is the number of receivers and $\tau_m(s)$ represents the calculated TDBS at position s. In addition, σ^2 represents the variance of errors in the TDBS caused by the perturbed SSP, the uncertainty at the receiver position and the errors from the cross correlation of the measured time series of the recorded data [15]. In accordance with reciprocity theory, $\tau_m(s)$ can be replaced by exchanging the unknown source and a given receiver to decrease the computational cost. In particular, the number of the hydrophones is chosen to be two in the present method. In addition, for the TDBS extracted at each single hydrophone based on Equation (7), the phase mismatch between two hydrophones could be neglected.

3. Simulation results

The performance of the TDBS method is shown in a numerical simulation, in which the sea bottom is assumed to be flat with a depth of 4000 m. The adopted SSP was measured in the South China Sea, as shown in Figure 1b. The depths of the sources are selected to be 10 m and 200 m, and the horizontal distances are assumed to be 15 km and 25 km from the hydrophones. Two hydrophones at depths of 510 and 820 m are used to obtain the time delay between the BS and SB paths, respectively. On the basis of the core data, the sound speed of the compressional wave and the density and attenuation coefficient of the sediment are 1550 m/s, 1.31 kg/m^3 and 0.15 dB/λ, respectively. The BELLHOP model [16] was used to compute the TDBS at each receiver and extract the time arrival information in the replica acoustic field. Furthermore, the standard deviation of errors σ was calculated as [15]

$$\sigma = \sqrt{\sigma_{rp}^2+\sigma_{ssp}^2+\sigma_{cross}^2}, \tag{7}$$

where $\sigma_{rp} = 2$ ms with the receiver position uncertainty of 3 m, $\sigma_{ssp} = 0$ ms because of the independent deep ocean waveguide, and $\sigma_{cross} = 1$ ms corresponding to the errors from the cross

correlation of different lengths of measured signals. As a result, $\sigma = \sqrt{2^2 + 1^2 + 0^2} \approx 2,24$ ms.

In the first scenario, the two receivers are deployed at the range of 25 km from the source. The TDBS matching results for a single receiver at a position of (200 m, 25 km) with different source depths are shown in Figures 2c and 2d. In other words, the number of the hydrophones is assumed to be one in Equation (7). Assuming that the measured time delay and the positions of the receivers are fixed, the estimated source depths at different horizontal ranges are determined as the main lobes shown in Figure 2c and 2d. The main lobes are oriented obliquely with respect to the range and depth axes in both figures. Obviously, the curvature of the main lobes decreases with the decrease in receiver depth at close range, and the slope of the main lobes approximates a constant at large range. Therefore, a linear relationship is approximated between the TDBS and the receiver depth/range at the large range, which is consistent with the aforementioned Equation (6). Furthermore, the width of the main lobes broadens as the range increases. This result indicates that the performance of the TDBS method degrades at large distance. Based on ray theory, the difference in depth between two rays launched with adjacent take-off angles is shown as

$$\Delta z = J\, \mathrm{d}\theta_0 / \cos\theta, \tag{8}$$
$$J = r\sqrt{\left(\frac{\partial z}{\partial \theta}\right)^2 + \left(\frac{\partial r}{\partial \theta}\right)^2},$$

where J and $\mathrm{d}\theta_0$ present the Jacobian and the difference in adjacent angles, respectively. Obviously, Δz increases with the increase in range for given take-off angles. In other words, the "ray tube" widens qualitatively at large distances.

The estimated ambiguity surfaces by using the TDBSs of the two receivers and Equation (7) are shown in Figures 3a-d, where the source positions represented by white squares are (15 km, 10 m), (15 km, 200 m), (25 km, 10 m) and (25 km, 200 m), respectively. The results indicate that the source position can be estimated effectively in the above-mentioned cases. It is worth noting that the estimated source position in Figure 3d is the intersection of the two main lobes shown in Figure 2c and 2d. Obviously, the localization performance is better at a closer range whether the source depth is 10 m or 200 m. A comparison of localization with the source at different depths is shown in Figure 3c and 2d. The results indicate a relatively good range localization capability for a shallow source and good depth localization capability for a deep source. Furthermore, the main lobes in the ambiguity surfaces are oriented toward the horizontal direction as the source depth increases. This finding can be interpreted that the calculated TDBS decreases with the hydrophone at a large depth for the given source position shown in Figure 2a and 2b.

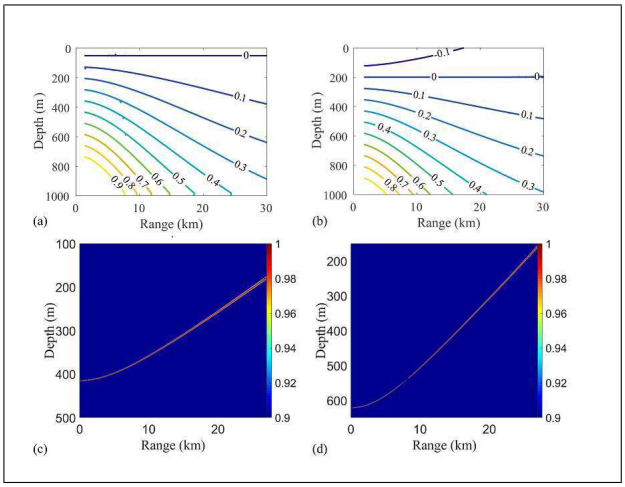

Figure 2. Simulated TDBSs on a hydrophone at depths of (a) 50 m and (b) 200 m under different source localizations. Ambiguity surfaces of the TDBS processing for a source at a position of (200 m, 25 km), where the hydrophones are at depths of (c) 510 m and (d) 820 m.

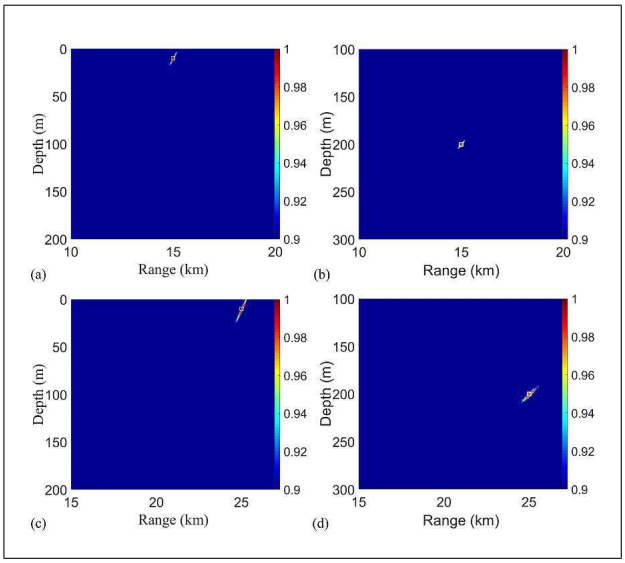

Figure 3. Ambiguity surfaces of the TDBS method for the source positions of (a) (15 km,10 m), (b) (15 km,200 m), (c) (25 km,10 m) and (d) (25 km,200 m), which are represented as white squares.

4. Experimental verification

A total of 16 distributed hydrophones were used to collect acoustic data during an experiment conducted in August 2014 in the South China Sea. The hydrophones were configured with a sample rate of 48 kHz and a sensitivity of −180 dB re 1 V/μPa. The hydrophones were deployed at 110–820 m with different intervals. The bathymetry of the deep ocean region was flat and the depth was approximated to be 4000 m. Broadband explosive sources with 1 kg TNT were used and deployed from the research ship whose GPS positions were recorded. The SSP in the water was measured with a conductivity-temperature-depth probe (CTD) near the position of the hydrophones, as shown in Figure 1b. For simplicity, the 15th and 16th hydrophones were selected at depths of 510 m and 820 m, respectively. Two groups of explosive source signals at ranges of 16.5 km and 17.5 km away from the receivers were chosen for demonstrating the performance of the TDBS method. On the basis of the characteristics of the bubble period of the explosive sources, the source depths were recalibrated as 58 m and 320 m [11]. Furthermore, the σ was assumed to be of the same value as in the simulation.

Figure 4a shows two received time series and the corresponding multipath time delay arrivals of the two hydrophones at depths of 510 m and 820 m, for the source at a position of (17.5 km, 320 m) in the experiment. For obtaining the measured TDBS, the time sequences containing only the SB and BS arrivals were selected. By using the cross-correlation method for the sequences [10], the time delays between BS and SB paths were extracted as 0.1071 s and 0.2843 s, which are the peak values represented as red squares in Figures 4b-c. The multipath

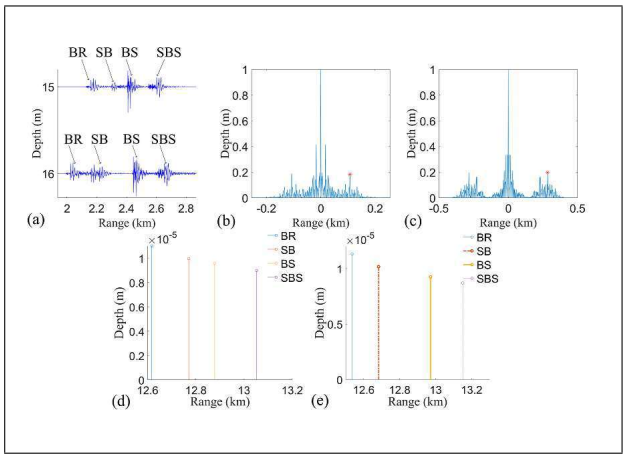

Figure 4. Results of the measured signals in the experiment: (a) measured signals at each hydrophone. (b-c) cross correlation process for the measured signals at the 15th and 16th hydrophones. (d-e) multipath time delays computed by BELLHOP at the 15th and 16th. hydrophones.

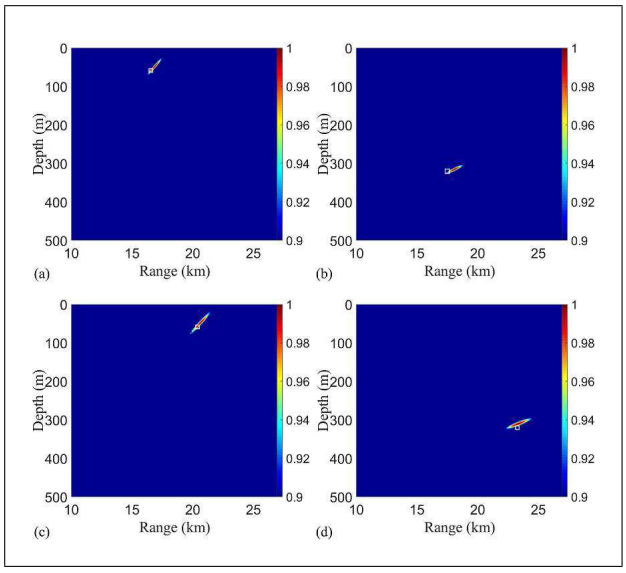

Figure 5. Ambiguity surfaces of the TDBS method for the source positions of (a) (16.5 km, 58 m), (b) (17.5 km, 320 m), (c) (20.38 km, 58 m) and (d) (23.26 km, 320 m), which are represented as white squares.

time delays, including the BR, SB, BS and SBS paths plotted in sequence, can be obtained from BELLHOP using the measured SSP and are shown in Figures 4d-e. The resulting replica TDBSs were 0.1075 s and 0.2883 s. The difference in the TDBS between the experiment data and the model result is small. The errors of the difference can be caused by the different lengths of the time windows for the recorded data, and the uncertainty of the environmental parameters and receiver depths.

The ambiguity surfaces were calculated by substituting the extracted TDBSs and the variance of errors in the TDBS into Equation (9) for different source positions, as shown in Figure 5. The results indicate that the source position can be estimated with a high resolution by the TDBS method. The errors between the peaks on the ambiguity surface and the real source positions were less than 10 m and 0.5 km in depth and range, respectively. Similarities between the experimental and the simulated results in the depth and range resolution for different source depths were also observed. The TDBS is more sensitive to the depth change when the receiver depth is closer to the source depth, and vice versa. The higher depth resolution and the lower range resolution could be achieved with a smaller distance between the source and the receiver depths, and vice versa. To a certain extent, the performance of the TDBS matching method is better at close range. The modeled TDBSs were greater than the measured ones for the source at a position of (17.5 km,320 m). Therefore, the real source position was in front of the peak of the main lobe shown in Figure 5b. Furthermore, the localization error may be caused by neglecting factors such as sound speed fluctuations, rough bottom, and surface and bottom scattering.

5. Conclusion

In summary, a source localization method based on the time delay between BS and SB arrivals in the deep ocean was proposed. The source position including range and depth can be localized by matching the measured and modeled TDBSs, which are calculated from two receivers at different depths. The performance of the TDBS method was demonstrated with the numerical simulation and the experimental data for different source position scenarios. The estimated source positions are in good agreement with the recalibrated depth and the GPS measurement in the experiment. The higher depth resolution and the lower range resolution could be achieved with a smaller distance between the source and the receiver depths, and vice versa. Compared with the source localization method that utilized the TDOA based on the D-SR arrivals, the proposed method could be applied in the first shadow zone. Furthermore, the TDBS method neglect the phase mismatch between two hydrophones, and needs no prior information about the broadband source. However, the BS and SB paths are closely related to the sediment properties, especially for the bathymetry. The variation of the bathymetry could reduce the robustness of the TDBS method due to the inaccurate estimated TDBSs. In other side, the BS and SB arrivals extracted from the received signals need to be identified, which are related to the difference of the depths between the source and the receivers. The large receiver depth can be a good choice for localizing the source in the shallow areas, which can neglect identifying the nature of the various arrivals. Further analysis would be helpful in improving the robustness of the method and applying it in ocean acoustics.

Acknowledgement

This work was supported by the Fundamental Research Funds for the Central Universities (Grant No. 3102018jcc033 and Grant No. 3102018bzc001)

References

[1] L. Tenorio-Hallé, A. M. Thode, J. Sarkar, et al.: A double-difference method for high-resolution acoustic tracking using a deep-water vertical array. J. Acoust. Soc. Am. **142** (2017) 3474–3485.

[2] C. O. Tiemann, A. M. Thode, J. Straley, et al.: Three-dimensional localization of sperm whales using a single hydrophone. J. Acoust. Soc. Am. **120** (2006) 2355–2365.

[3] J. Gebbie, M. Siderius, J. S. Allen III: A two-hydrophone range and bearing localization algorithm with performance analysis. J. Acoust. Soc. Am. **137** (2015) 1586–1597.

[4] R. Mccargar, L. M. Zurk: Depth-based signal separation with vertical line arrays in the deep ocean. J. Acoust. Soc. Am. **133** (2013) EL320–E325.

[5] G. P. Kniffin, J. K. Boyle, L. M. Zurk, M. Siderius: Performance metrics for depth-based signal separation using deep vertical line arrays. J. Acoust. Soc. Am. **139** (2016) 418–425.

[6] R. Duan, K. D. Yang, Y. L. Ma, et al.: Moving source localization with a single hydrophone using multipath time delays in the deep ocean. J. Acoust. Soc. Am. **136** (2014) EL159–EL165.

[7] E. K. Skarsoulis, S. E. Dosso: Linearized two-hydrophone localization of a pulsed acoustic source in the presence of refraction: Theory and simulations. J. Acoust. Soc. Am. **138** (2015) 2221–2234.

[8] Z. X. Lei, K. D. Yang, Y. L. Ma: Passive localization in the deep ocean based on cross-correlation function matching. J. Acoust. Soc. Am. **139** (2016) EL196–EL201.

[9] K. D. Yang, Q. L. Yang, X. L. Guo, R. Cao: A simple method for source depth estimation with multi-path time delay in deep ocean. Chin Phys Lett. **33** (2016) 124302.

[10] Q. L. Yang, K. D. Yang: Sound source depth estimation based on multipath time delay in deep water. Acta Acust United Ac. **104** (2018) 363–368.

[11] J. B. Weng, Y. M. Yang: Experimental demonstration of shadow zone localization using deep water interference patterns measured by a single hydrophone. IEEE J. Ocean Eng. **99** (2017) 1–8.

[12] R. Duan, K. D. Yang, Y. L. Ma: Narrowband source localisation in the deep ocean using a near-surface array. J. Acoust Aust. **42** (2014) 36–42.

[13] F. B. Jensen, W. A. Kuperman, M. B. Porter, et al.: Computational ocean acoustics. AIP press, New York, 2011.

[14] L. M. Brekhovskikh, Y. P. Lysanov: Fundmentals of ocean acoustics. AIP press, New York, 2003.

[15] E. M. Nosal, L. N. Frazer: Sperm whale three-dimensional track, swim orientation, beam pattern and click levels observed on bottom-mounted hydrophones. J. Acoust. Soc. Am. **122** (2007) 1969–1978.

[16] M. B. Porter, H. P. Bucker: Gaussian beam tracing for computing ocean acoustic fields. J. Acoust. Soc. Am. **82** (1987) 1349–1359.